POLITECNICO DI TORINO
Repository ISTITUZIONALE

A Flexible Virtual Synchronous Machine for Four-Wire Inverters Supplying Three-Phase and Single-Phase Systems

Original
A Flexible Virtual Synchronous Machine for Four-Wire Inverters Supplying Three-Phase and Single-Phase Systems / Camboni, A., Roveri, A., Mandrile, F., Bojoi, R.. - (2026), pp. 1-6. (2026 Energy Conversion Congress & Expo Europe (ECCE Europe) Valencia (Spa) 14-18 September 2026) [10.1109/ecceeurope67962.2026.11737974].

Availability:
This version is available at: 11583/3017869 since: 2026-11-16T12:28:07Z

Publisher:
IEEE

Published
DOI:10.1109/ecceeurope67962.2026.11737974

Terms of use:

This article is made available under terms and conditions as specified in the corresponding bibliographic description in the repository

Publisher copyright
IEEE postprint/Author's Accepted Manuscript

©2026 IEEE. Personal use of this material is permitted. Permission from IEEE must be obtained for all other uses, in any current or future media, including reprinting/republishing this material for advertising or promotional purposes, creating new collecting works, for resale or lists, or reuse of any copyrighted component of this work in other works.

(Article begins on next page)

21 November 2026

A Flexible Virtual Synchronous Machine for Four-Wire Inverters Supplying Three-Phase and Single-Phase Systems

Alessia Camboni
Dipartimento Energia "G.Ferraris"
Politecnico di Torino
Torino, Italy
alessia.camboni@polito.it

Alessandro Roveri
Prima Electro S.P.A.
Moncalieri, Italy
alessandro.roveri@primaelectro.com

Fabio Mandrile
Dipartimento Energia "G.Ferraris"
Politecnico di Torino
Torino, Italy
fabio.mandrile@polito.it

Radu Bojoi
Dipartimento Energia "G.Ferraris"
Politecnico di Torino
Torino, Italy
radu.bojoi@polito.it

***Abstract*—This paper proposes a Virtual Synchronous Machine (VSM) control suitable for four-wire grid-connected converters. The proposed VSM-4W control features a single virtual rotor, three independent virtual electrical circuits (i.e., a three-phase stator), and three excitation controllers, enabling per-phase voltage/reactive power regulation. The virtual rotor mechanically couples the three virtual circuits, thus preserving a common inertial response. The advancement of this solution lies in its operation under arbitrary phase imbalance and split-phase conditions, as well as in multi-single-phase networks. In addition, this control structure allows the VSM to support the grid even when supplying independent single-phase systems. The proposed VSM-4W is experimentally validated under abrupt grid reconfigurations, including single-phase and split-phase operations, asymmetric faults, and frequency perturbations under unbalanced voltages. The experimental results demonstrate the high adaptability of the proposed solution to arbitrary grid conditions while providing the ancillary services typical of VSM algorithms.**

***Index Terms*—Virtual Synchronous Machine (VSM), Four-Wire Inverters, Grid Support**

I. Introduction

The increasing electrification of both generation and loads is driving a structural transition of power systems toward inverter-dominated power grids. Besides, interest in battery energy storage systems is rising, both at the grid scale and for small electrical islands, thereby replacing conventional diesel generators. In this latter case, 4-wire converters are used [1], since they must be able to operate in three-phase mode or supply multiple single-phase networks or standalone single-phase loads.

Besides supplying loads, grid-tied converters are now required to contribute to power-system services naturally provided by synchronous machines [2], such as inertial response, frequency support, and dynamic voltage/reactive power regulation. To this purpose, the concept of Virtual Synchronous Machine (VSM) addresses these needs by emulating an alternator in the converter controller [3], [4].

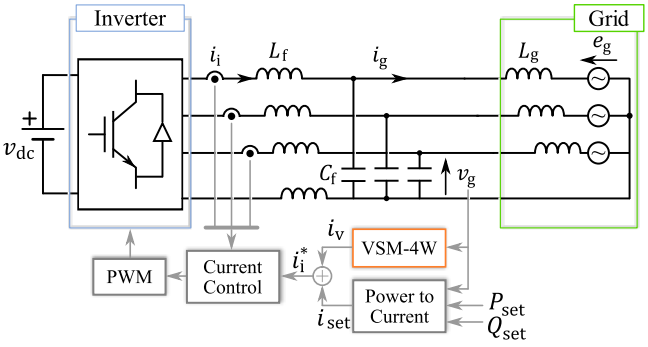


Fig. 1. Schematic representation of a four-leg grid-tied inverter equipped with the proposed VSM solution.

However, most VSM solutions are typically intended for three-phase, three-wire systems operating in symmetrical conditions [4]. For four-wire converters, available control approaches often rely on sequence decomposition to preserve positive-sequence behaviour and mitigate the impact of negative- and zero-sequence components [5]. To this end, dedicated controllers are implemented for positive-sequence voltage behavior under unbalanced loads [6]–[9]. While such methods can improve voltage symmetry under moderate imbalance, they are primarily designed to restore balance rather than to operate in generic four-wire scenarios. In such scenarios, one or two phases may be absent or differ significantly from each other (e.g., single-phase operation, split-phase configurations, phase-to-ground faults, or two open phases), rendering balanced system restoration unlikely.

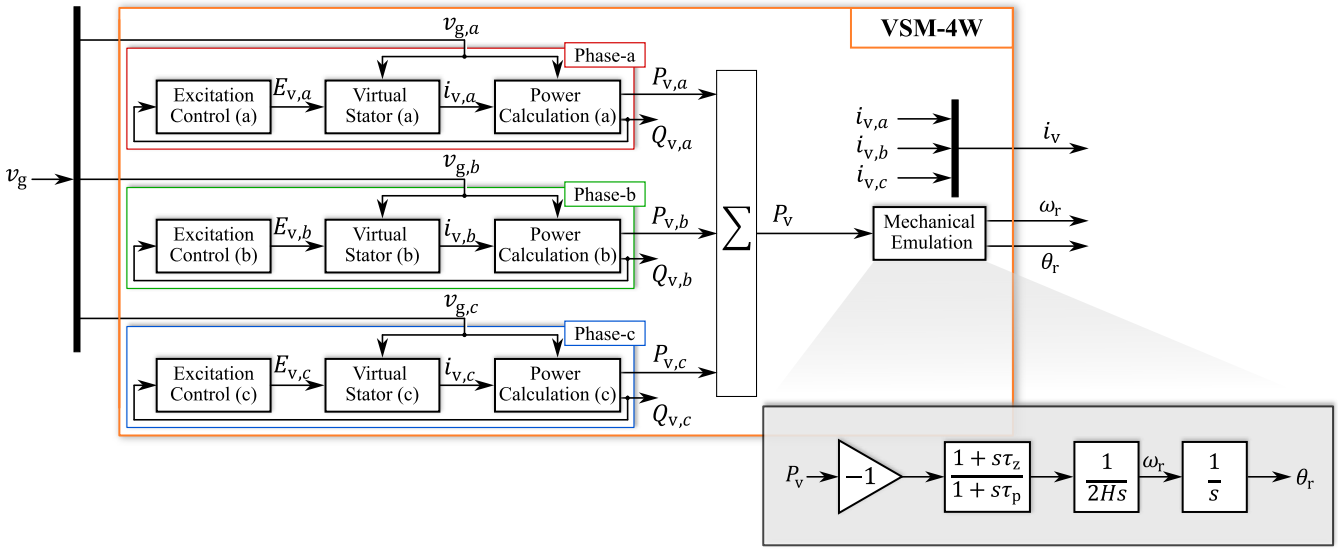


Fig. 2. Schematic representation of the proposed VSM-4W algorithm.

Although the VSM concept is well established in the literature [10], its application to four-leg converters remains only partially explored. In particular, the literature lacks VSM-based algorithms that support highly unbalanced conditions (e.g., single-phase and split-phase configurations) without relying solely on positive-sequence modeling or negative/zero-sequence suppression.

Therefore, this paper proposes a flexible VSM algorithm, explicitly designed for four-wire converters, based on a single virtual rotor coupled to three independent virtual electrical circuits (i.e., a three-phase stator) and three excitation controllers. In this structure, each phase is controlled as a single-phase virtual circuit, allowing for an independent regulation of its voltage and reactive power. Furthermore, the common virtual rotor maintains a unified inertial response and synchronization mechanism, while removing the structural dependency on the balanced three-phase assumption.

The VSM-4W algorithm is experimentally validated on a 4-wire converter under abrupt grid reconfigurations, including single-phase and split-phase operation, asymmetric faults, frequency perturbations, and voltage sags, demonstrating the robustness and adaptability of the proposed solution.

The rest of the paper is organized as follows. Section II presents the implemented control, with a focus on the VSM model for four-wire inverters. Section III provides the experimental results, demonstrating the high adaptability of the proposed control. Section IV concludes the paper.

II. Proposed Control

The system under study, shown in Fig. 1, consists of a four-leg inverter, connected to the grid via an LC filter. The four inverter legs are designed identically, as are the filter inductances at the inverter output. The grid is represented as a voltage source e_{g} in series with the line inductance L_{g}. Moreover, the voltage across the filter capacitor is denoted v_{g}.

The implemented algorithm operates as a Virtual Synchronous Compensator (VSC) [11], characterized by two main blocks in parallel: the Power-to-Current (PC) and the proposed VSM-4W blocks [11]. The steady-state power references P_{set} and Q_{set} are applied via the PC block and are set by a higher-level control (e.g., Maximum Power Point Tracking (MPPT)). The PC block outputs are the three-phase setting currents denoted as i_{set}.

In contrast, the VSM-4W model operates at a zero-power reference and responds only to grid perturbations, providing ancillary services (e.g., inertial response and reactive power support) [11]. Therefore, the VSM-4W outputs (i.e., three-phase virtual currents i_{v}) are zero in steady-state. The PC and VSM-4W blocks are combined by summing i_{set} and i_{v} and applying the sum to a current regulator, as shown in Fig. 1. The current regulator utilizes a Proportional-Resonant (PR) controller, with the controlled current at the inverter output i_{i}.

A. VSM-4W Model

The proposed VSM-4W model, represented in Fig. 2, consists of three decoupled electrical circuits (i.e., a three-phase stator), each equipped with an excitation control. A virtual rotor (i.e., the mechanical emulation) mechanically couples the electrical circuits.

In more detail, each electrical circuit defines a virtual current $i_{\mathrm{v},i}$, and behaves as a Thévenin equivalent with a virtual impedance $\bar{Z}_{\mathrm{v},i}$. Note that the virtual impedances are set equal in the three phases $\left(\text{i.e., } \bar{Z}_{\mathrm{v},a} = \bar{Z}_{\mathrm{v},b} = \bar{Z}_{\mathrm{v},c} = R_{\mathrm{v}} + jsL_{\mathrm{v}}\right)$. As in single-phase algorithms [12], the electrical equations for each phase are represented in an auxiliary $\alpha\beta-$frame, where the β component is derived by rotating the α component by $\pi/2$. In $\alpha\beta-$frame, the electrical equations for the $i-$th phase can be expressed as in (1) and (2), whereas the active

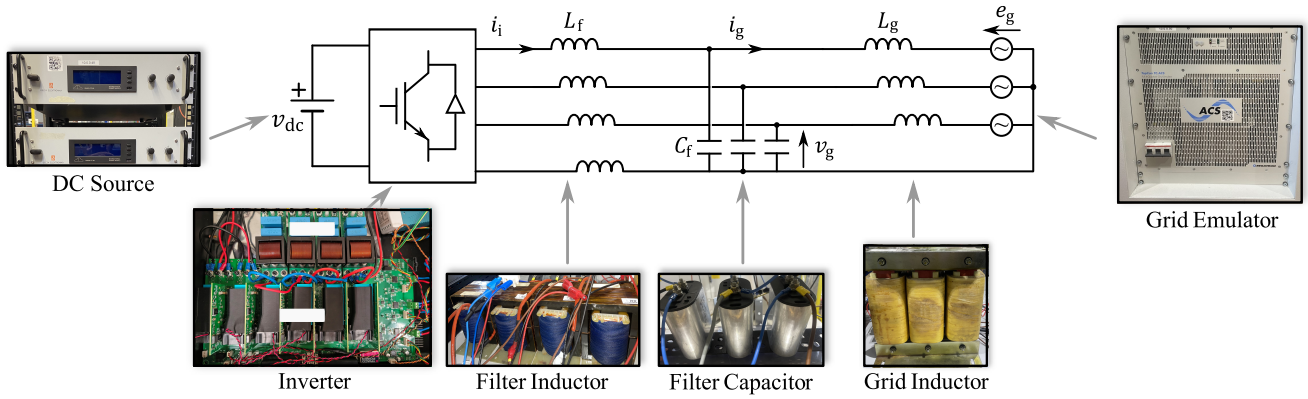


Fig. 3. Experimental setup.

and reactive virtual powers are calculated as in (3) and (4), respectively. Note that the virtual voltage is considered aligned with the α component (i.e., $e_{v\alpha,i} = E_{v,i}\cos(\theta_i)$, $e_{v\beta,i} = -E_{v,i}\sin(\theta_i)$) [12].

$$e_{v\alpha,i} - v_{g\alpha,i} = R_v i_{v\alpha,i} + L_v \frac{di_{v\alpha,i}}{dt} \tag{1}$$

$$e_{v\beta,i} - v_{g\beta,i} = R_v i_{v\beta,i} + L_v \frac{di_{v\beta,i}}{dt} \tag{2}$$

$$P_{v,i} = v_{g\alpha,i} i_{v\alpha,i} + v_{g\beta,i} i_{v\beta,i} \tag{3}$$

$$Q_{v,i} = v_{g\beta,i} i_{v\alpha,i} - v_{g\alpha,i} i_{v\beta,i} \tag{4}$$

As illustrated in Fig. 2, three excitation control blocks set the virtual voltage amplitude of the three phases, each based on its virtual reactive power $Q_{v,i}$. The dynamics of the excitation control are defined by (5), where the time constant T_e and gain k_e are equal across the three phases and tuned according to [13].

$$\frac{d\Delta E_{v,i}}{dt} = -\frac{\omega_r k_e}{T_e} Q_{v,i} \tag{5}$$

Moreover, the virtual active powers for each phase are summed to yield a total power, P_v, which is used in the mechanical emulation [11]. As shown in Fig. 2, the lead-lag damping proposed in [14] is implemented for the mechanical part, where H is the inertial time constant and τ_z and τ_p are designed as in [14]. Therefore, the three electrical circuits are coupled via the virtual rotor (i.e., via the mechanical equation), thus obtaining the virtual rotor frequency, ω_r, and the rotor angle θ_r as in (6).

$$\frac{d\theta_r}{dt} = \Delta\omega_r + \omega_0 \tag{6}$$

Note that rotor angle θ_r coincides with the electrical angle of phase$-a$ (i.e., $\theta_a = \theta_r$), whereas $\theta_b = \theta_a - \varphi_b$ and $\theta_c = \theta_a - \varphi_c$. Indeed, φ_b and φ_c need to be calculated since the control can operate under unbalanced conditions (i.e., $\theta_a - \theta_b \neq \theta_b - \theta_c \neq 2\pi/3$). For example, φ_b and φ_c are zero when the three phases are aligned. To this end, the tangent of φ_b can be expressed as in (7) using the trigonometric expression for $\sin(\theta_a - \theta_b)$ and $\cos(\theta_a - \theta_b)$.

$$\begin{aligned}\tan(\varphi_b) &= \frac{\sin(\theta_a - \theta_b)}{\cos(\theta_a - \theta_b)} = \\ &= \frac{\sin(\theta_a)\cos(\theta_b) - \cos(\theta_a)\sin(\theta_b)}{\sin(\theta_a)\sin(\theta_b) + \cos(\theta_a)\cos(\theta_b)}\end{aligned} \tag{7}$$

The expression in (7) results in (8) considering the quadrature relation of the quantities in the $\alpha\beta-$frame. Note that (8) can be applied since $|v_{g\alpha,i}| = |v_{g\beta,i}|$, thereby simplifying the voltage amplitude.

$$\tan(\varphi_b) = \frac{v_{g\alpha,a} v_{g\beta,b} - v_{g\beta,a} v_{g\alpha,b}}{v_{g\alpha,a} v_{g\alpha,b} + v_{g\beta,a} v_{g\beta,b}} \tag{8}$$

The VSM-4W outputs are the three-phase virtual currents, for which only the α component is applied (i.e., $i_{v,i} = i_{v\alpha,i}$).

B. Power-to-Current Block

For the PC-block, the $i-$th current reference $i_{set,i}$ is calculated as in (9) by combining the active and reactive power equations in $\alpha\beta-$frame. The $i-$th power reference can be defined separately or divided equally between the phases (e.g., $P_{set,i} = P_{set}$ and $Q_{set,i} = Q_{set}$) [15].

$$i_{set,i} = i_{set,\alpha,i} = \frac{P_{set,i} v_{g\alpha,i} + Q_{set,i} v_{g\beta,i}}{|v_{g,i}|^2} \tag{9}$$

The proposed three-phase stator increases the control robustness and modularity while enabling proper operation under highly unbalanced conditions and phase-to-ground faults.

III. Experimental Validation

The proposed solution is tested in the experimental setup shown in Fig. 3. A DC source supplies a four-wire, two-level, GaN-based inverter, connected to a grid emulator via an LC filter. A three-phase inductor is included in series as line impedance. The code for the experimental validation is generated in PLECS, and an RT Box platform is used to control the inverter. The base power is 3.8 kVA, and the switching frequency is 50 kHz. The main control and system parameters are summarized in Table I.

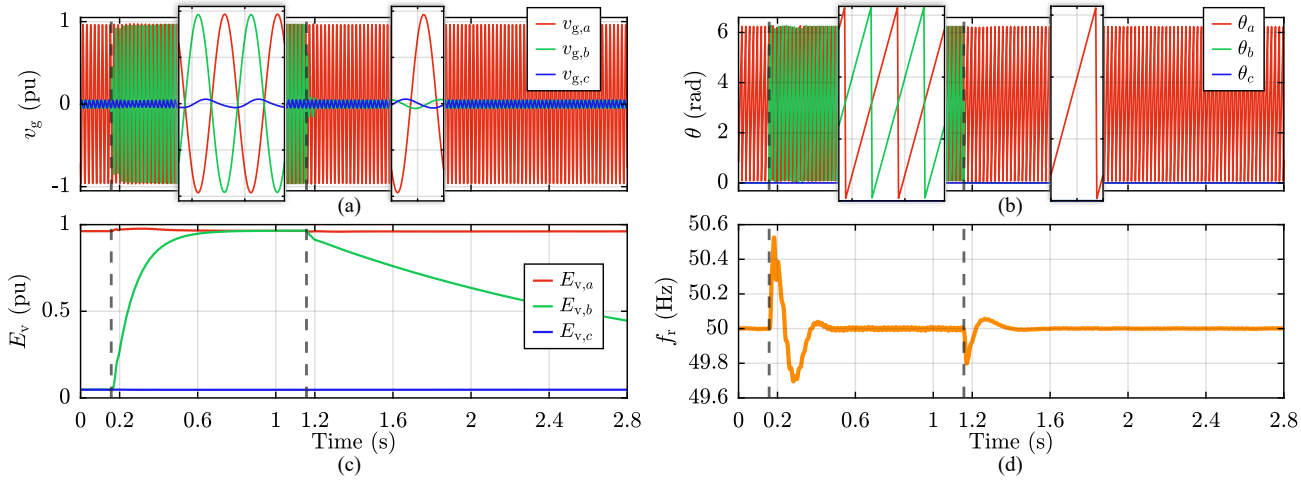


Fig. 4. Experimental results for a grid configuration change from single-phase with $v_{g,b} = v_{g,c} \approx 0$ pu to split-phase conditions with $v_{g,b} = -v_{g,a}$: (a) three-phase voltage v_g, (b) control angles θ_{abc}, (c) virtual voltage amplitudes $E_{v,abc}$, and (d) virtual rotor frequency f_r.

TABLE I
SYSTEM AND CONTROL PARAMETERS.

Inverter		**Base Values**		**Grid**	
S_N	3.8 kVA	S_{base}	3.8 kVA	$\widehat{E}_g$	$120\sqrt{2}$ V
f_{sw}	50 kHz	V_{base}	$120\sqrt{2}$ V	L_g	0.077 pu
		ω_{base}	314 rad/s V		
VSM				**LC Filter**	
L_v	0.2 pu	k_e	1.5 pu	L_f	2 mH
R_v	0.04 pu	T_e	0.1 s	C_f	22 μF
H	4 s	τ_z	0.113 s		
		τ_p	0.019 s		

The following tests are carried out to evaluate the performance of the proposed VSM-4W control:

- Change in grid configuration from a single-phase to a split-phase condition;
- Frequency variation under highly unbalanced conditions;
- Voltage sag under highly unbalanced conditions;
- Asymmetric fault with balanced three-phase pre-fault and post-fault conditions.

The VSM-4W model is expected to manage unbalanced conditions thanks to the three-phase stator structure. As the proposed algorithm is VSM-based, it is expected to provide ancillary services during grid perturbations (e.g., inertial response and fault current) even under unbalanced conditions.

A. Single-phase and Split-Phase conditions

The proposed control is tested for abrupt changes in the grid configuration, and Fig. 4 depicts the experimental results. During the first 0.2 s, the control is synchronized for a single-phase condition with $v_{g,b} = v_{g,c} \approx 0$ pu. For the single-phase condition, $|e_{g,b}|$ and $|e_{g,c}|$ are set to 0.05 pu in the grid emulator to account for its control limitations. Then, a split-phase condition is applied, where $v_{g,b} = -v_{g,a}$. As shown in Figs. 4b and 4c, the control synchronize to the split-phase

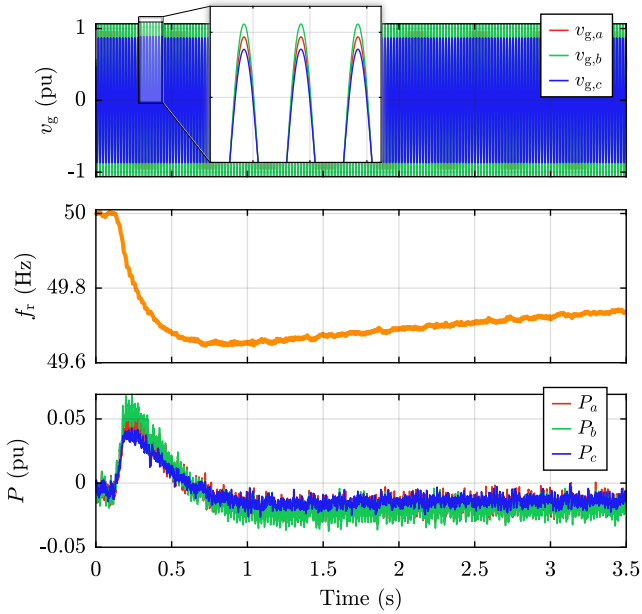


Fig. 5. Experimental results for a frequency perturbation under unbalanced conditions with voltage amplitudes $|v_{g,a}| = 1$ pu, $|v_{g,b}| = 1.1$ pu, and $|v_{g,c}| = 0.9$ pu. From top to bottom: three-phase voltage v_g, virtual rotor frequency f_r, and active powers P_{abc}.

configuration, and the virtual voltage amplitude $E_{v,b}$ increases according to the time constant T_e. Next, the grid is restored in a single-phase configuration. Consequently, $E_{v,b}$ decreases, while the virtual rotor changes to synchronize with the single-phase condition.

Thanks to the three virtual circuits, the proposed control can maintain synchronism and operate correctly even under single-phase and split-phase grid conditions.

B. Frequency Variation

The second test consists of a frequency perturbation, applied when the system operates under highly unbalanced

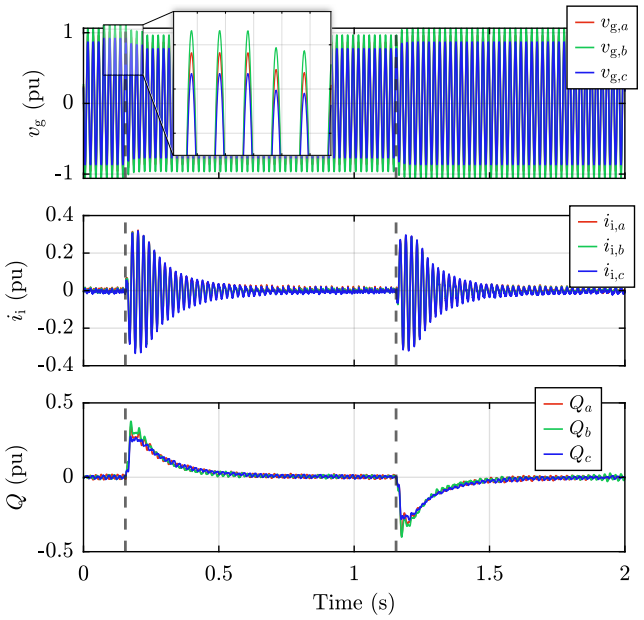


Fig. 6. Experimental results for a voltage sag of 0.1 pu under unbalanced conditions with pre-fault voltage amplitudes $|v_{g,a}| = 1$ pu, $|v_{g,b}| = 1.1$ pu, and $|v_{g,c}| = 0.9$ pu. From top to bottom: three-phase voltage v_g, three-phase output inverter current i_i, and reactive powers Q_{abc}.

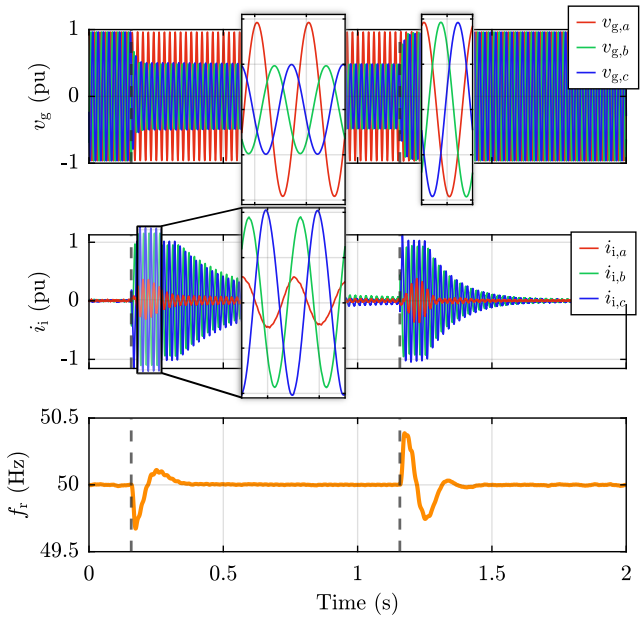


Fig. 7. Experimental results for an asymmetric voltage sag of $|v_{g,a}| = 1$ pu, $|v_{g,b}| = 0.5$ pu, and $|v_{g,c}| = 0.5$ pu with balanced three-phases pre-fault conditions. From top to bottom: three-phase voltage v_g, three-phase output inverter current i_i, and virtual rotor frequency f_r.

conditions (i.e., when the three-phase voltages are aligned in phase). Note that the three-phase voltages differ in amplitude ($|v_{g,b}| > |v_{g,a}| > |v_{g,c}|$). When the frequency varies, the proposed control supports the grid by injecting inertial power (i.e., P_v increases) even under unbalanced conditions. In more detail, the inertial power is distributed among the three phases according to the voltage amplitude (i.e., $|v_{g,b}| > |v_{g,a}| \Rightarrow P_{v,b} > P_{v,a}$), thus resulting in equal exploitation of the inverter's leg current capability.

C. Voltage Sag

A voltage sag is applied for the same grid configuration as in Section III-B (i.e., aligned three-phase voltages). Fig. 6 shows the experimental results, in which the voltage amplitudes are reduced by 0.1 pu in each phase for 1 s. In pre-fault conditions, no power is exchanged with the grid. At the fault occurrence, the VSM control injects a fault current through the virtual current i_v, whose amplitude depends on the virtual impedance and the applied voltage sag. As shown in Fig. 6, the excitation control determines a reactive power injection at the fault occurrence (i.e., when $E_{v,i} > V_{g,i}$), which persists until the virtual voltage settles (i.e., depends on the time constant T_e).

D. Asymmetric Fault

Next, the control is tested in three-phase balanced conditions when an asymmetrical fault is applied with $|v_{g,b}| = |v_{g,c}| = 0.5$ pu for 1 s. The main experimental results are depicted in Fig. 7. Due to voltage variation, the currents of phases b and c rapidly increase to 1 pu, at which their amplitudes are saturated. Similarly to Section III-C, the VSM-4W control settles into the asymmetric fault conditions according to the time constant of the excitation controllers. Then, the pre-fault condition is restored, and the control correctly synchronizes to the three-phase balanced condition, as shown in Fig. 7.

Therefore, the proposed VSM-4W model synchronizes under highly unbalanced conditions and abrupt changes in grid configuration while providing ancillary services (i.e., inertial response and reactive power support).

IV. Conclusion

This paper proposes a four-wire Virtual Synchronous Machine (VSM-4W) control strategy for 4-wire converters, enabling flexible operation under arbitrary grid conditions while providing ancillary services to the grid.

To properly operate under highly unbalanced conditions, this approach combines a single virtual rotor (mechanical emulation) with three decoupled single-phase electrical circuits (i.e., a three-phase stator) and excitation controllers. This structure decouples the voltage/reactive power behavior in each phase while preserving a unified inertial response through the common rotor.

The experimental results demonstrated that the proposed controller maintains synchronism and adapts coherently to abrupt grid reconfigurations, including single-phase and split-phase operation. Even under highly unbalanced conditions, the proposed VSM-4W can provide inertial power for frequency variations and inject fault current to support the grid during voltage sags. Moreover, the active and reactive power support is distributed among the phases in proportion to the voltage grid amplitude.

Therefore, the proposed VSM-4W extends VSM's applicability to practical four-wire scenarios where single-phase

and strongly unbalanced conditions are intrinsic and cannot be effectively addressed by enforcing balanced three-phase operation.

REFERENCES

[1] F. Rojas, R. Cárdenas, C. Burgos-Mellado, E. Espina, J. Pereda, C. Pineda, D. Arancibia, and M. Díaz, "An overview of four-leg converters: Topologies, modulations, control and applications," *IEEE Access*, vol. 10, pp. 61 277–61 325, 2022.

[2] nationalgridESO, "Compliance Guidance Notes for NOA Stability Compensation Service Phase 2," National Grid Electricity System Operator Limited, Tech. Rep., Warwick, West Midlands, U.K, November 2021.

[3] J. Liu, Y. Miura, and T. Ise, "Comparison of dynamic characteristics between virtual synchronous generator and droop control in inverter-based distributed generators," *IEEE Transactions on Power Electronics*, vol. 31, no. 5, pp. 3600–3611, 2015.

[4] Z. Huang, Z. Liu, G. Shen, K. Li, Y. Song, and B. Su, "A virtual synchronous generator-based control strategy and pre-synchronization method for a four-leg inverter under unbalanced loads," *Symmetry*, vol. 16, no. 9, 2024.

[5] G. Tan, Y. Zheng, W. Zhao, L. Qi, and X. Sun, "Droop control of three- and four-leg hybrid parallel inverters based on three-phase generalized coordinate transformation," *IEEE Transactions on Power Electronics*, vol. 39, no. 12, pp. 15 831–15 844, 2024.

[6] J. Wang, F. Luo, B. Gu, Z. Ji, Z. Lv, and T. Wang, "Improved control strategies for three-phase four-leg virtual synchronous generator with unbalanced loads," in *2017 19th European Conference on Power Electronics and Applications (EPE'17 ECCE Europe)*, 2017, pp. P.1–P.10.

[7] B. Sharma, P. K. Pankaj, Y. Terriche, A. Saim, A. Shrestha, C.-L. Su, and J. M. Guerrero, "Power sharing in three-level npc inverter based three-phase four-wire islanding microgrids with unbalanced loads," *IEEE Access*, vol. 11, pp. 20 725–20 740, 2023.

[8] B. F. Brown, J. Westman, J. Enslin, and Z. Zhang, "Development of a two-level, four-leg smart inverter for microgrid applications," in *2024 IEEE 15th International Symposium on Power Electronics for Distributed Generation Systems (PEDG)*, 2024, pp. 1–6.

[9] J. Sun, Z. Liu, C. Xu, Q. Gu, and J. Fu, "Approximate optimal voltage-support control with minimum unbalance factor considering zero-sequence voltage in four-wire faulty weak grid," *Electric Power Systems Research*, vol. 249, p. 112005, 2025. [Online]. Available: https://www.sciencedirect.com/science/article/pii/S0378779625005966

[10] M. Chen, D. Zhou, and F. Blaabjerg, "Modelling, implementation, and assessment of virtual synchronous generator in power systems," *Journal of Modern Power Systems and Clean Energy*, vol. 8, no. 3, pp. 399–411, 2020.

[11] F. Mandrile, E. Carpaneto, and R. Bojoi, "Grid-feeding inverter with simplified virtual synchronous compensator providing grid services and grid support," *IEEE Transactions on Industry Applications*, vol. 57, no. 1, pp. 559–569, 2021.

[12] J. A. Suul, S. D'Arco, and G. Guidi, "Virtual synchronous machine-based control of a single-phase bi-directional battery charger for providing vehicle-to-grid services," *IEEE Transactions on Industry Applications*, vol. 52, no. 4, pp. 3234–3244, 2016.

[13] F. Mandrile, E. Carpaneto, E. Armando, and R. Bojoi, "Simple tuning method of virtual synchronous generators reactive control," in *2020 IEEE Energy Conversion Congress and Exposition (ECCE)*. IEEE, 2020, pp. 2779–2785.

[14] F. Mandrile, V. Mallemaci, E. Carpaneto, and R. Bojoi, "Lead-lag filter-based damping of virtual synchronous machines," *IEEE Transactions on Industry Applications*, vol. 59, no. 6, pp. 6900–6913, 2023.

[15] I. Aizpuru, A. Davila, E. Planas, J. A. Cortajarena, and J. L. Martin, "Phase-independent control of a three-phase four-leg inverter," in *2023 IEEE 32nd International Symposium on Industrial Electronics (ISIE)*. IEEE, 2023, pp. 1–6.